Electronic Supplementary Information (ESI) for

Reaction Pathways N-substituted Carbon Catalyst during the Electrochemical Reduction of Nitrate to Ammonia

Zheng Chen[§a], Jianhong Chen[§b], Giovanni Barcaro[c], Tetyana, M. Budnyak[b], Anna Rokicińska[d], Richard Dronskowski[a,e], Serhiy Budnyk[f], Piotr Kuśtrowski[d], Susanna Monti*[c], and Adam Slabon*[g]

[§]equal contribution

[a]Institute of Inorganic Chemistry, RWTH Aachen University, 52056 Aachen, Germany

[b]Department of Materials and Environmental Chemistry, Stockholm University, 10691 Stockholm, Sweden

[c] CNR-ICCOM−Institute of Chemistry of Organometallic Compounds, 56124 Pisa, Italy

[d]Faculty of Chemistry, Jagiellonian University, 30-387 Krakow, Poland

[e]Hoffmann Institute of Advanced Materials, Shenzhen Polytechnic, 7098 Liuxian Blvd, Shenzhen, China

[f]AC^{2}T research GmbH, Viktor-Kaplan-Str. 2c, 2700 Wiener Neustadt, Austria

[g]Inorganic Chemistry, University of Wuppertal, Gaußstr. 20, 42119 Wuppertal, Germany

Corresponding Authors

Adam Slabon: adam.slabon@mmk.su.se

Susanna Monti: susanna.monti@pi.iccom.cnr.it

Table of Contents

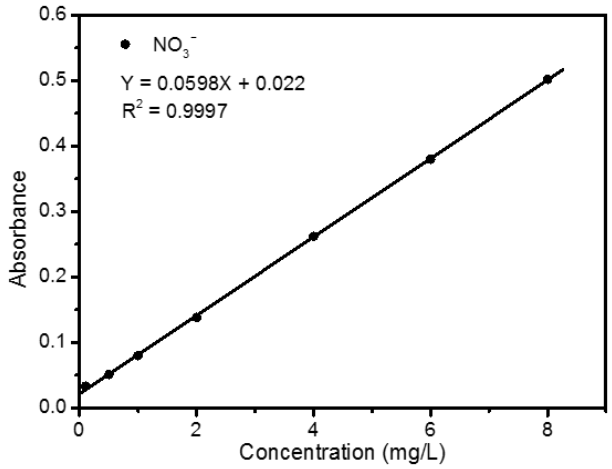

Fig. S1. The calibration curve of NO_3^- with good linearity.

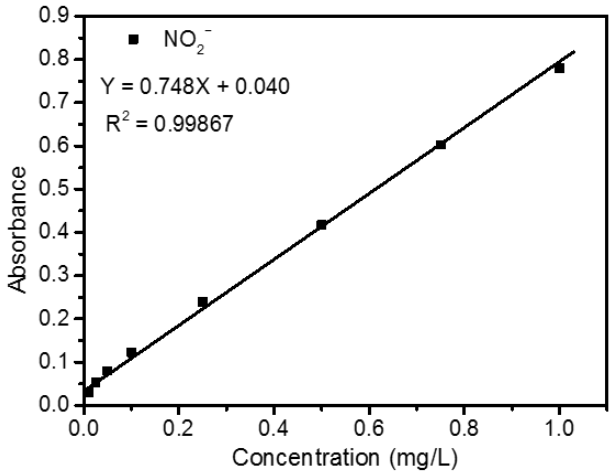

Fig. S2. The calibration curve of NO_2^- with good linearity.

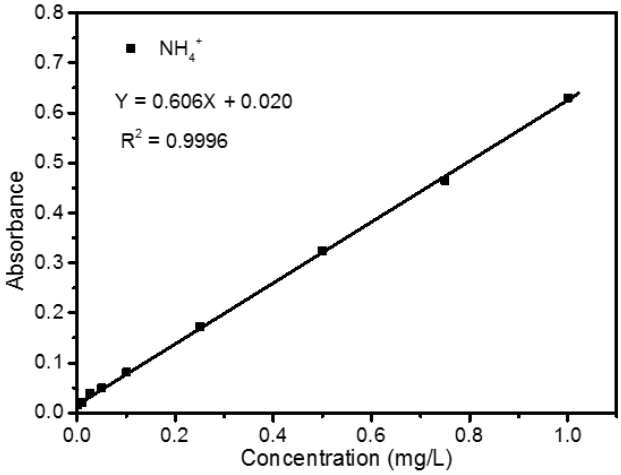

Fig. S3. The calibration curve of NH_4^+ with good linearity.

ReaxFF Molecular Dynamics (RMD) Simulations

Model building. The molecular model used as starting material consisted of cellulose fibers parallelly packed in a rectangular parallelepiped box. Eight cellulose fibers, made of sixteen chains with six-teen glucosyl residues each, arranged as a parallelepiped rod (84 × 25 × 25 $Å^3$), were assembled parallelly close to each other on two parallel planes (four fibers on each plane – Fig. S4) and used as the carbon source in the carbonization process.

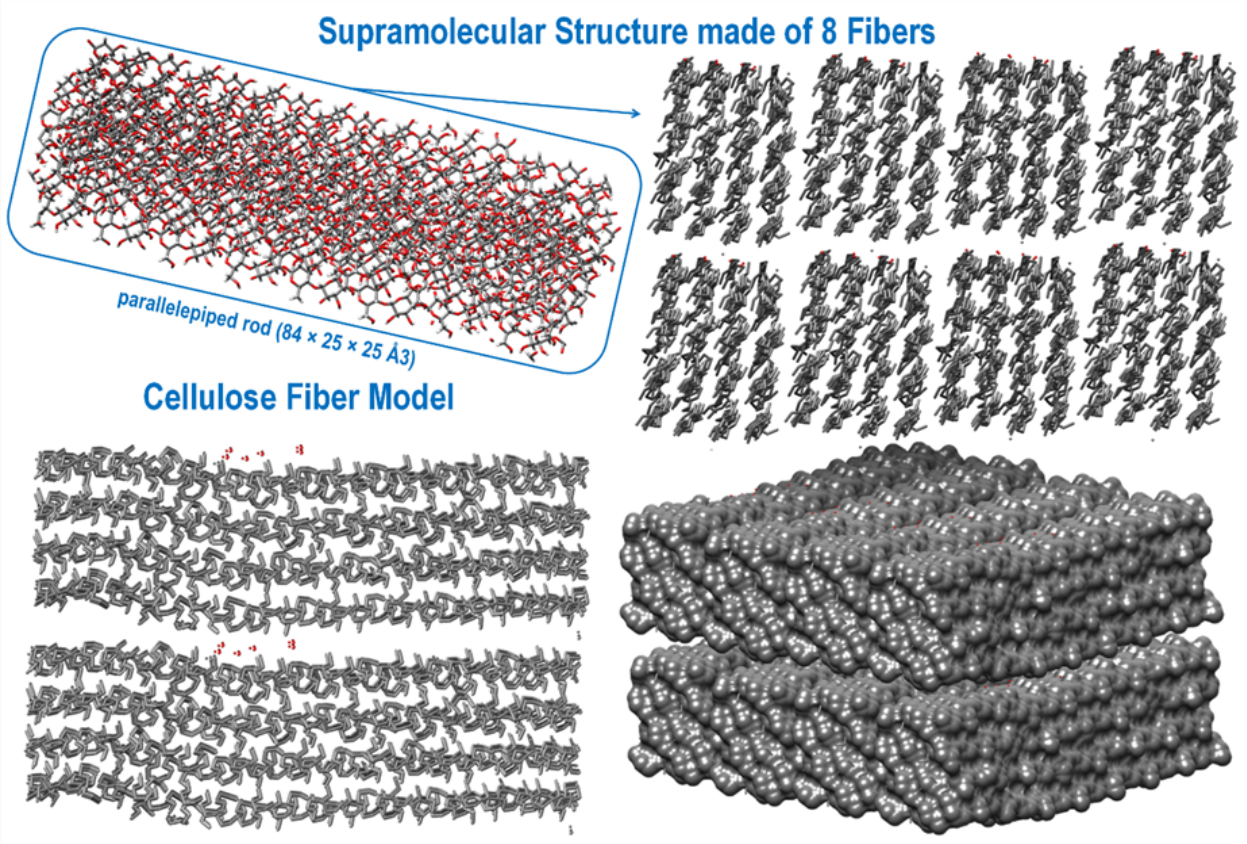

Fig. S4. The multi-fiber model used to start the cellulose carbonization simulations (stick and vdW representations – C gray, O red, H white). All the hydrogen and the oxygen atoms forming H_2O were removed to speed up the calculations.

Preliminary RMD simulations. The complete fiber (containing all carbon, oxygen, and hydrogen atoms) shown in Fig. S4 was used, first, to disclose, through reactive MD, the initial stages of the cellulose carbonization process in terms of reactions and type of products, to define an efficient less time-consuming computational strategy to carbonize bigger supramolecular models. The selected configuration was inserted in a larger box, and the temperature was increased from 0 to 1500 K in 50 ps. Then the system was maintained at that temperature for the rest of the simulation time (around 100 ps). During the dynamics, we observed the desorption

of H followed by the formation of H_2 (~1000 K), the release of OH groups, and the formation of H_2O and H_3O^+ (1500 K). These were then accompanied by the desorption of CO fragments. The progressively produced water molecules were removed from the simulation box to speed up the calculations. A complex porous carbon network started to shape from the sparse chains present in the cell. The final configuration consisted, essentially, of the carbon atoms (*backbone*) of the cellulose chains with a few oxygen atoms.

Given these premises, we decided to start the carbonization of the larger system from the reduced *backbone* model containing only the atoms that were not involved in water formation.

RMD Simulations of the carbonization and N-doping processes. The eight-fiber model shown in Fig. S1 was inserted in a 100 x 100 x100 $Å^3$ simulation box (periodic boundary conditions were applied in all directions), equilibrated at 300 K in the NVT ensemble, and then slowly heated to 600 K, in a time span of approximately 50 ps, slightly modulating the force field parameters[1] to randomize the cellulose chains, and kept there for about 50 ps (Fig. S5). Then, the heating process was repeated, increasing the temperature to 1200 K at a rate of 0.002 K/iteration (60 ps). A few nitrogen atoms were inserted in the simulation box to mimic the experimental oxidizing stage. The system was maintained at this temperature for about 500 ps to observe the reorganization of the structure (production stage – Fig. S6).

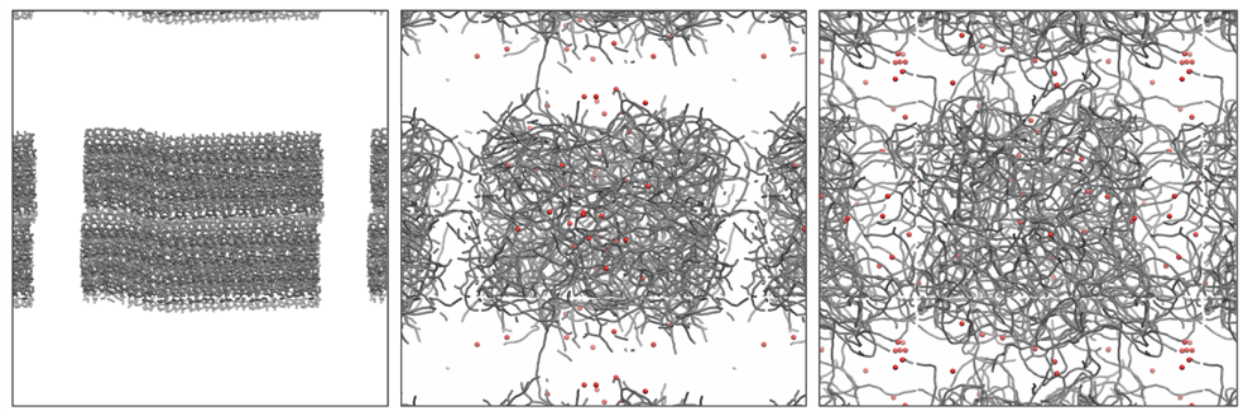

Fig. S5. Randomization simulation of the eight cellulose fibers (stick model with C gray and O red). Periodic replicas are shown to highlight the formation of continuous material Evolution of the structure from the beginning to the final structure.

The RMD simulations were based on a force field used earlier for these types of materials.[2]

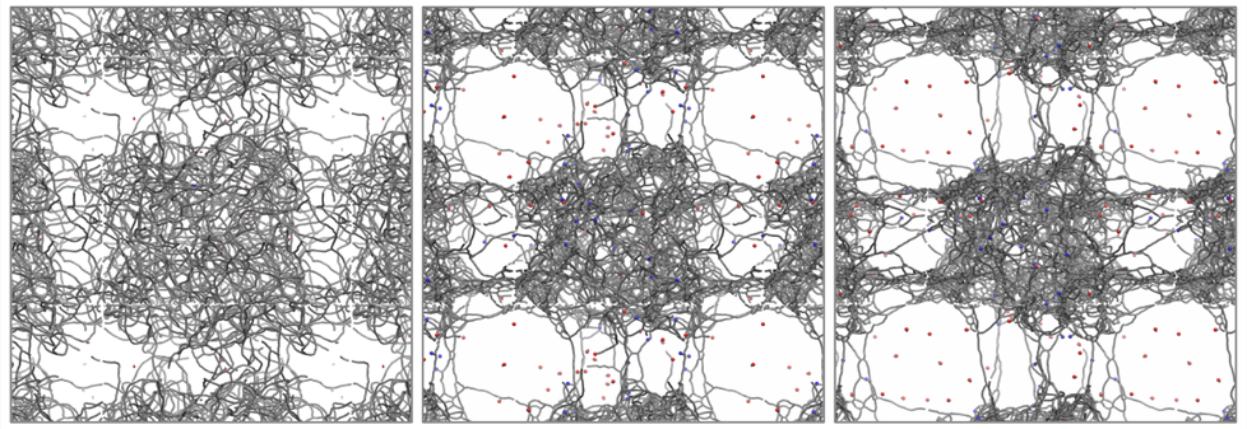

Fig. S6. Reorganization of the randomized fibers (stick model with C gray, O red, N blue). Periodic replicas are shown to highlight the formation of continuous material Evolution of the structure from the beginning to the final structure.

The time step was set to 0.2 fs, and the temperature was controlled through the Hoover-Nosé thermostat with a relaxation constant of 0.1 ps. All RMD runs were carried out with the ReaxFF code implemented in the Amsterdam Density Functional (ADF)/ReaxFF[3] and Large-scale Atomic/Molecular Massively Parallel Simulator (LAMMPs) packages.[4] From the production stage, a few configurations displaying amorphous carbon matrices with alternating graphitic sheet regions were extracted and used as initial geometries for the N-doping procedure. The models were surrounded by NH_3 and simulated at high temperatures (1200 K) to mimic nitrogen doping (Fig. S7).

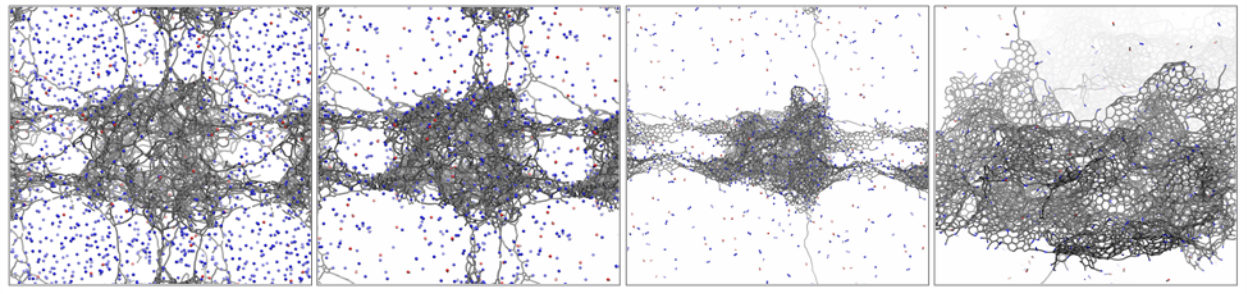

Fig. S7. Randomized N-doping of the last model obtained from the reconstruction simulations (stick model with C gray, O red, N blue). Periodic replicas are shown to highlight the formation of continuous material. Evolution of the structure from the beginning to the final structure.

To identify the most appropriate NH_3 concentration for obtaining modeling results comparable with the experimental data, we carried out three different simulations with different amounts of N atoms, namely 0.01, 0.02, and 0.04 (expressed as N/C ratio). This comparison was useful for estimating not only the capacity of adsorption but also various possible types of insertion (Fig. S8). The model corresponding to

the highest N concentration turned out to be the most promising, and it was selected for the subsequent simulations in solutions in the presence of NO_3^- ions.

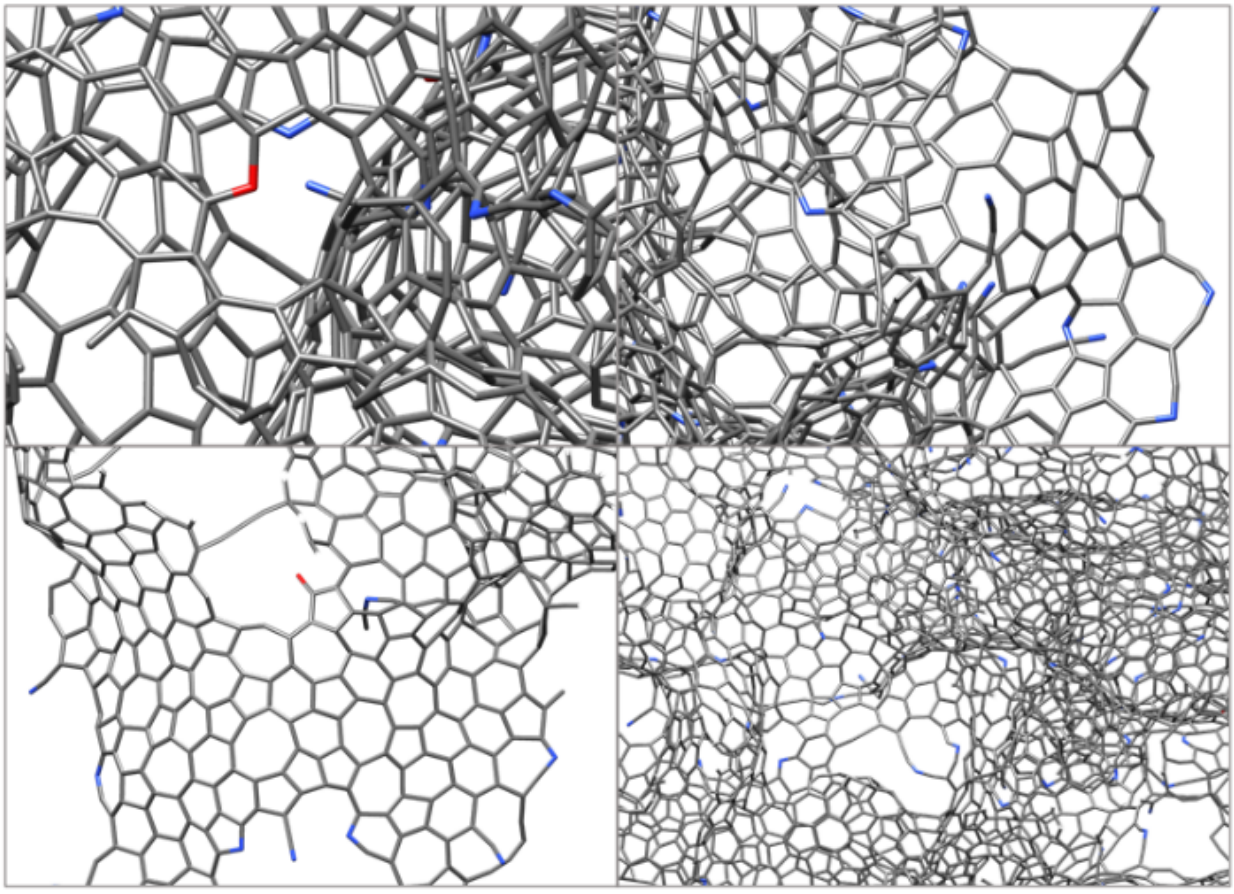

Fig. S8. Portions of the final model (stick model with C gray, O red, N blue) showing possible locations of the nitrogen atoms inserted during the doping procedure.

Characterization of the models. The pores of the NDC model structures were identified via the CAVER software.[5] The code resorts to spherical probes to fill void regions inside the selected configuration by changing the radius of the probe. The characterization of the generated molecular model in terms of pores is shown in Fig. S9, where we have separated the pore structure from the molecular model to give a clearer view of its extension and size.

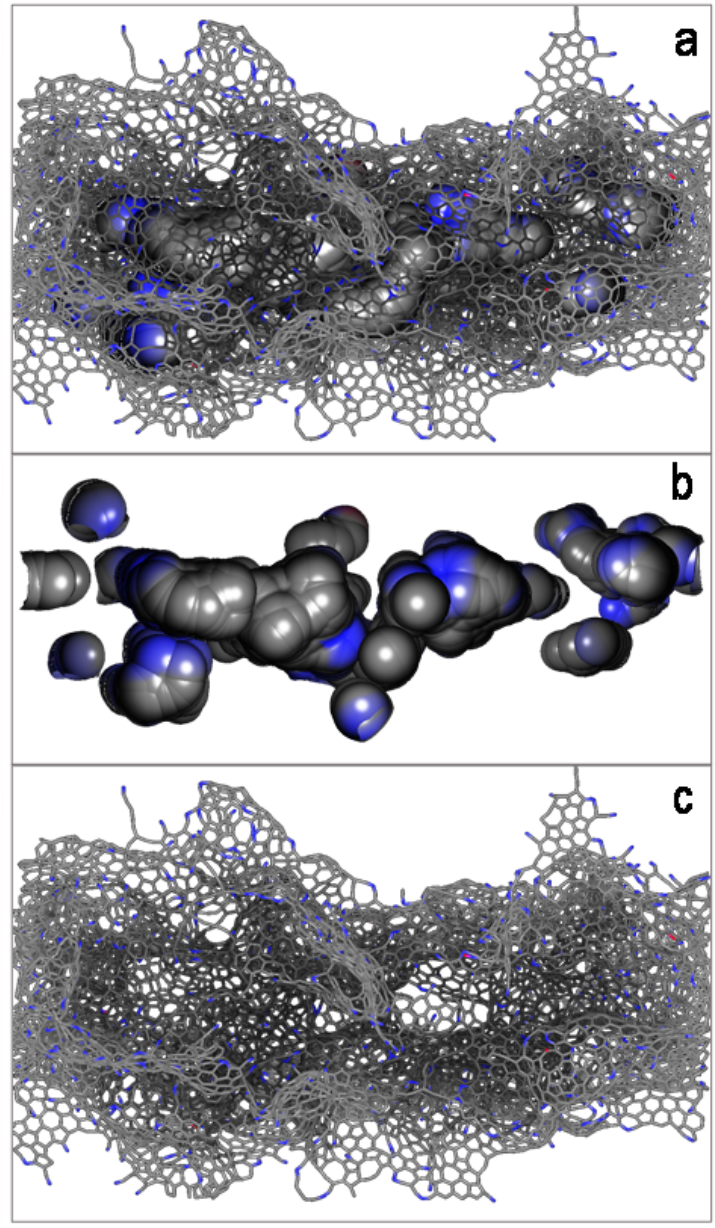

Fig. S9. a) complete model; b) organization of the cavities, tunnels, and pockets rendered through a combination of spheres, c) empty structure. The final model (stick model and sphere colored according to the atom type: C gray, O red, N blue) filled with CAVER's spheres. These were used to trace the tunnels and pockets that characterize the porous nature.

RMD simulations of the carbonized model surrounded by NO_3^- ions. RMD simulations were performed in the NVT ensemble, first, at 100 K (100 ps) and then, as production dynamics, at 300 K for about 300 ps. The chosen configuration was equilibrated at ambient temperature and surrounded by NO_3^- ions only to identify the preferential adsorption locations. This procedure helped stabilize the positions of the ions and explore various binding areas (Fig. S10).

Inspection of the final configuration revealed that the ions could be found all around the NDC model, in the pockets and tunnels, and had the tendency to bind to defect points and release their O atoms to the support (Fig. S11). To investigate this behavior further, we extracted a representative defective portion of the NDC, where one of these ions was adsorbed, and explored qualitatively possible reaction mechanisms using quantum chemistry calculations.

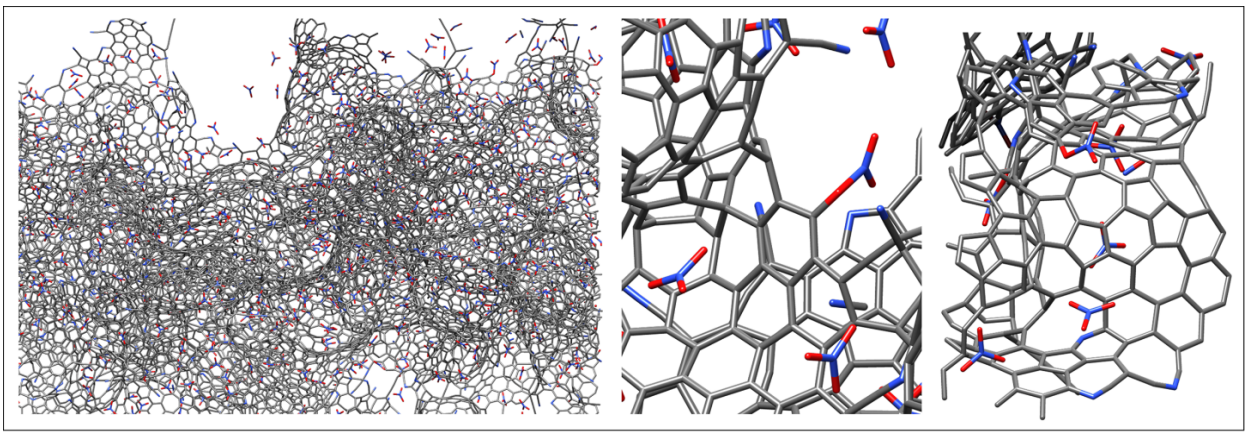

Fig. S10. The final model (stick model and sphere colored according to the atom type: C gray, O red, N blue) is surrounded by NO_3^- ions.

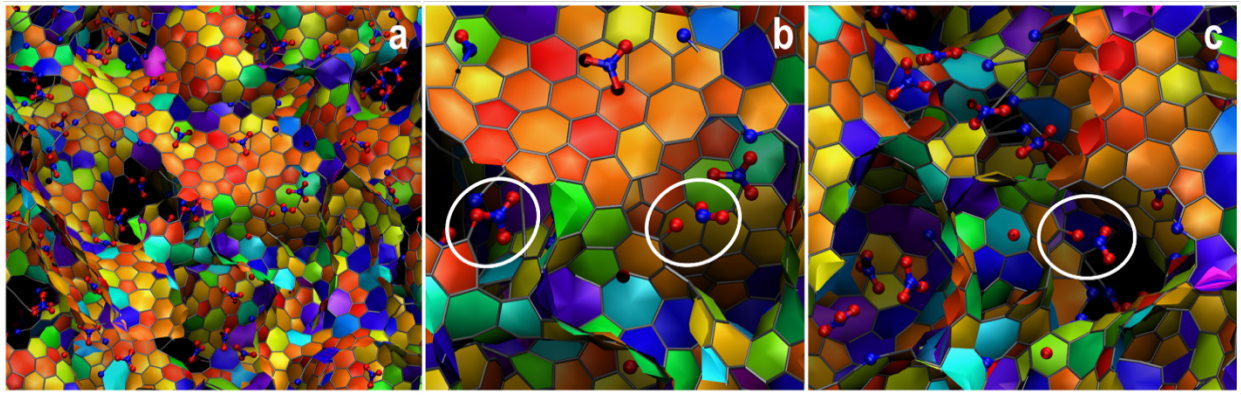

Fig. S11. Portions of the final model (stick/ball and stick representation with C gray, O red, N blue) where possible locations of the NO_3^- ions are shown. The rings of the NDC matrix are colored according to the number of bonds and planarity (VMD software). NO_3^- binding modes are highlighted in the circles.

Exploratory quantum chemistry optimizations. QC optimizations were carried out to identify possible adsorption modes of the NO_3^- ions to the defective region of the NDC support and their reactions there through the g09 software[6] using the B3LYP functional and the 6-31G* basis set.

The optimization path, depicted in Fig. S12, shows an initial configuration of the HNO_3 molecule that has already released the hydrogen to a carbon atom nearby and then releases two of its O to the support remaining connected to it.

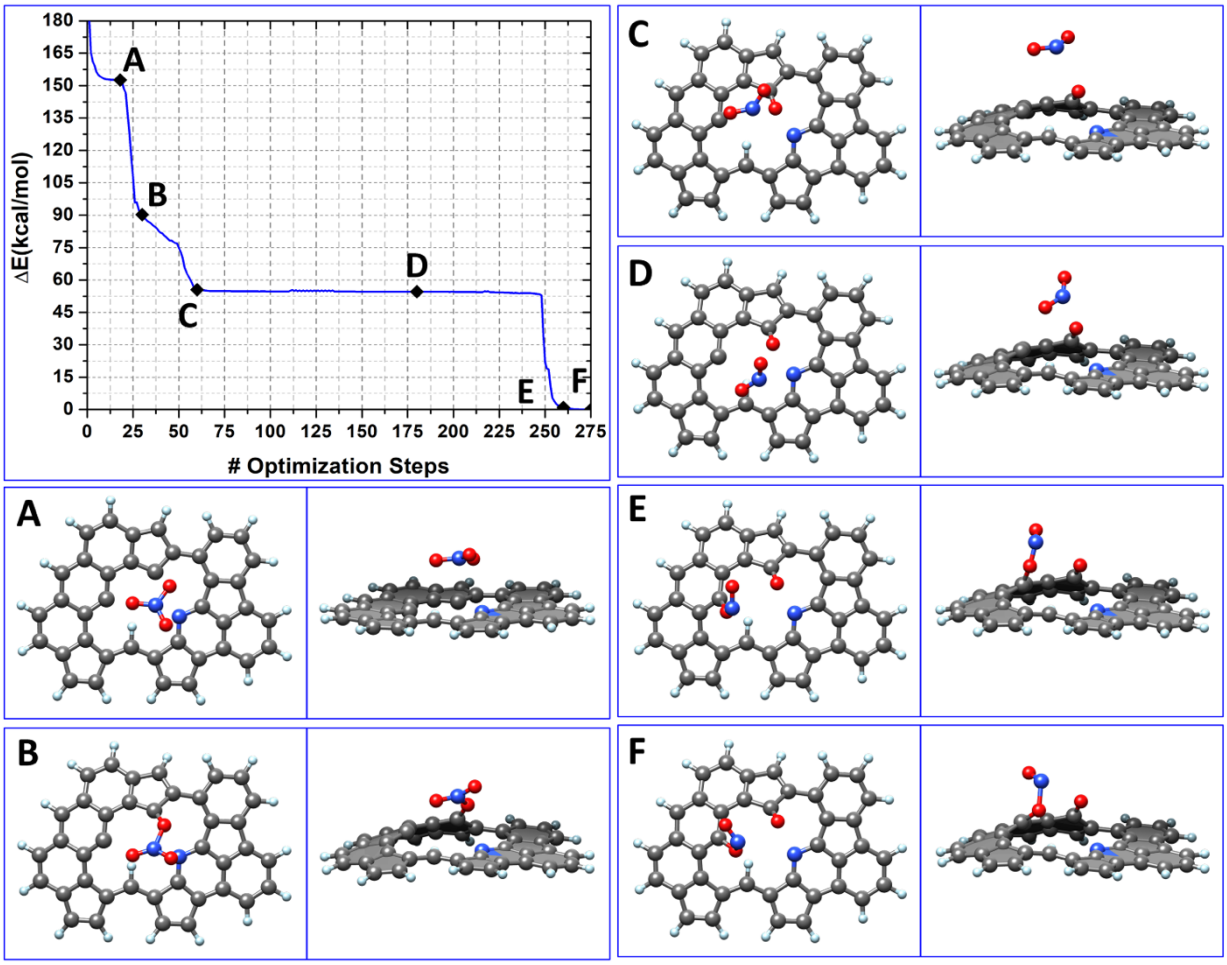

Fig. S12. Possible reaction mechanism obtained through the QC optimization of the NO_3^- ion positioned on a defective portion of the NDC support (extracted from the RMD simulations).

Then, we tried to evaluate possible adsorption modes through the oxygen (Fig. S13) or the nitrogen (Fig. S14) and reactions of NO with the support and the surrounding species, represented by a few water molecules.

NO-C connection (Fig. S13). The optimizations of the initial configurations A and C produced the final structures B and H, respectively, thus reproducing the final formation of NH_3/NH_4.

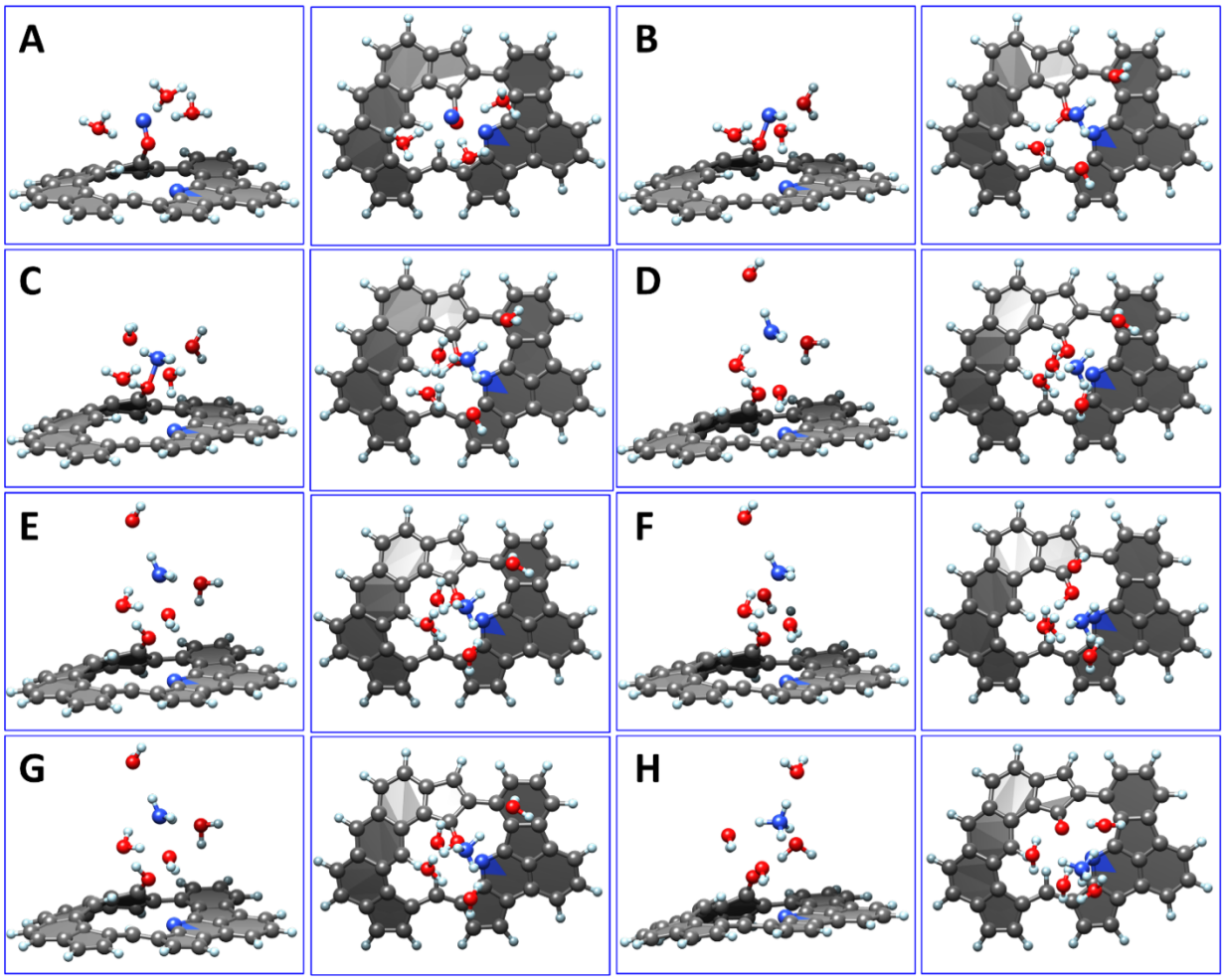

Fig. S13. Possible reaction mechanisms of NO, attached to the support through the O atom, with a few surrounding solvent molecules. These structures have been obtained through sequential QC optimizations.

ON-C connection (Fig. S14). The optimizations of the initial configuration A produced the final structure H with the formation of NH_3.

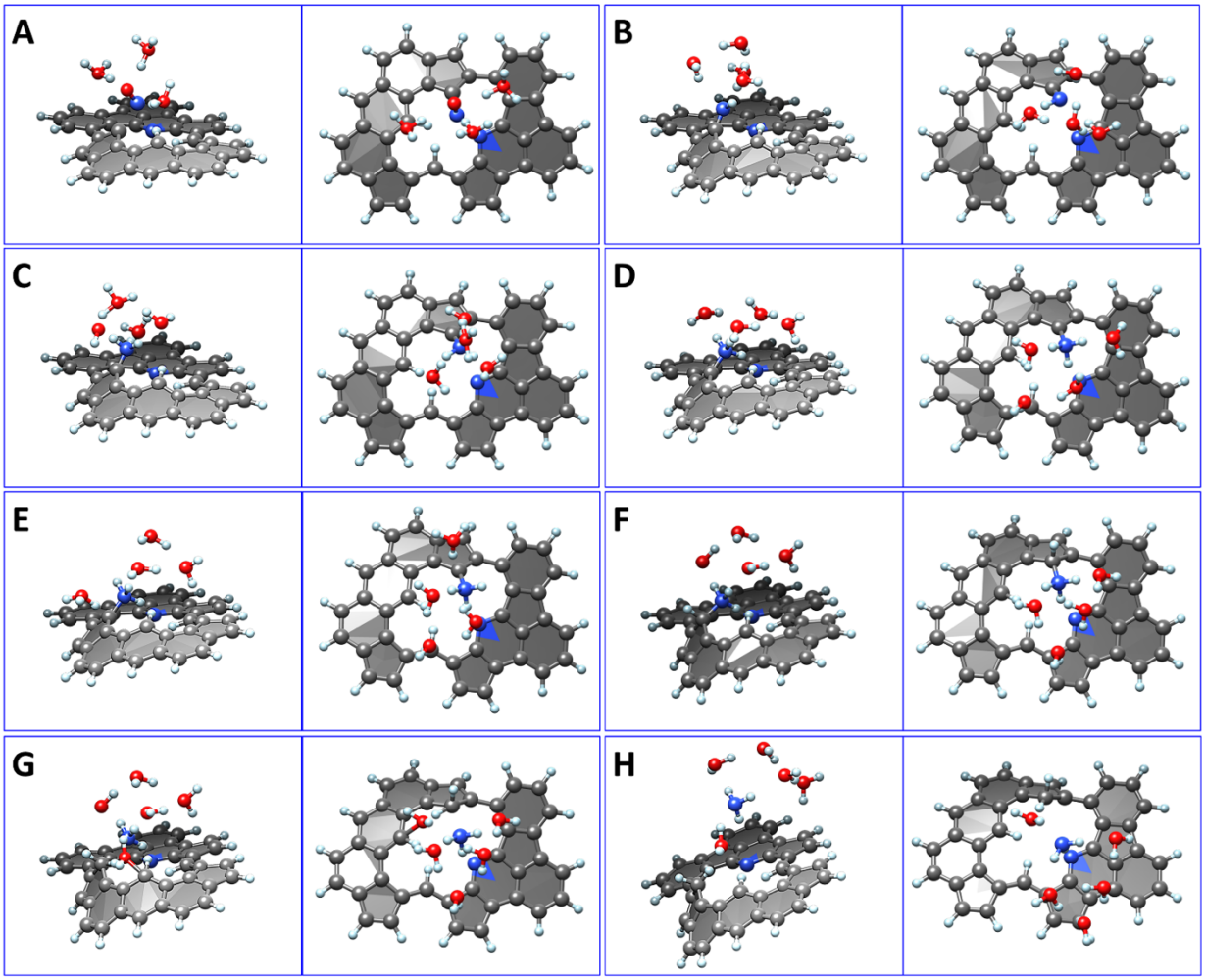

Fig. S14. Possible reaction mechanisms of NO, attached to the support through the N atom, with a few surrounding solvent molecules. These structures have been obtained through sequential QC optimizations.

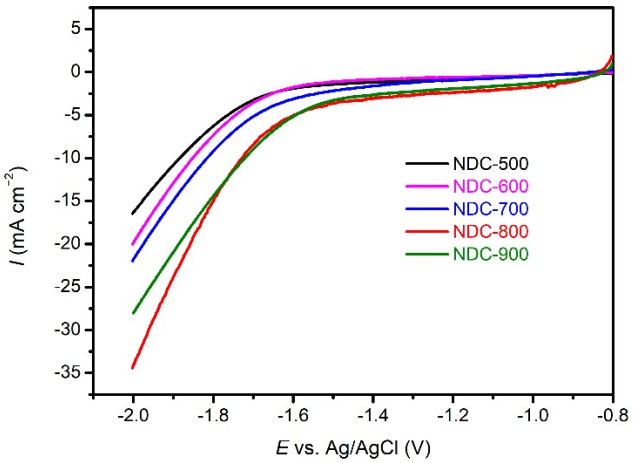

Fig. S15. LSV curves of NDC-500, NDC-600, NDC-700, NDC-800 and NDC-900 for HER in a 0.1 M NaOH (pH 13) electrolyte.

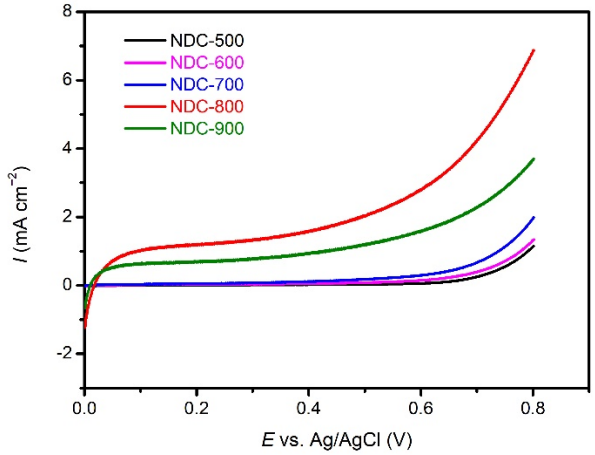

Fig. S16 LSV curves of NDC-500, NDC-600, NDC-700, NDC-800 and NDC-900 for OER in a 0.1 M NaOH (pH 13) electrolyte.

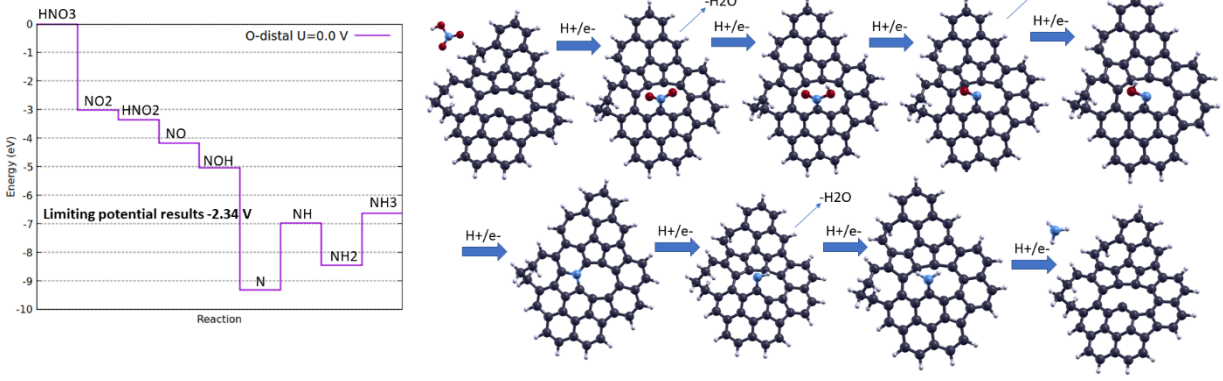
HNO3
O-distal U=0.0 V
NO2
HNO2
NO
NOH
NH
NH2
NH3
N
Limiting potential results -2.34 V
Energy (eV)
Reaction
H+/e-
-H2O

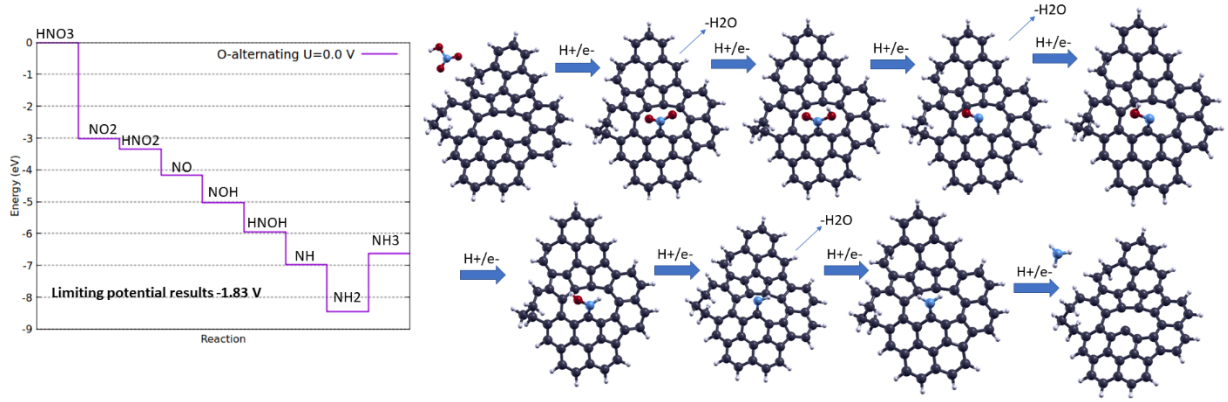
HNO3
O-alternating U=0.0 V
NO2
HNO2
NO
NOH
HNOH
NH
NH2
NH3
Limiting potential results -1.83 V
Energy (eV)
Reaction
H+/e-
-H2O

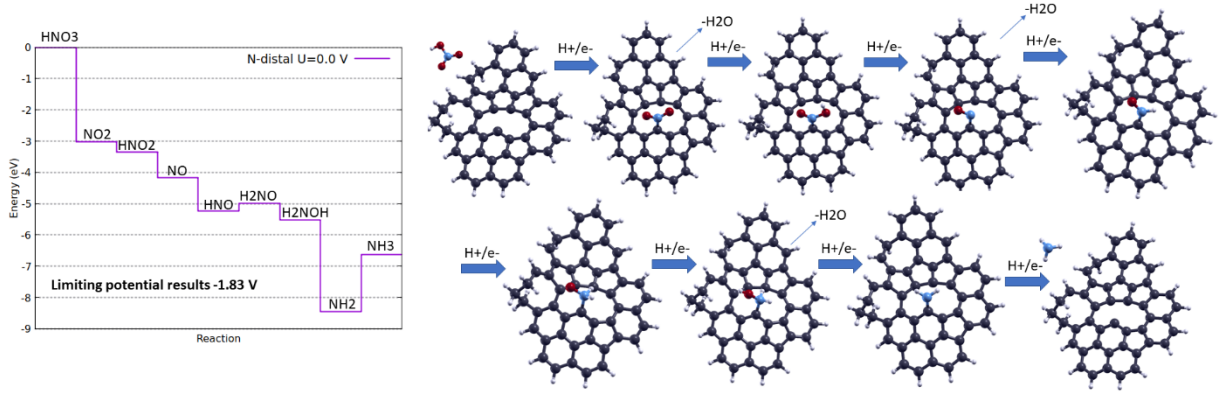
HNO3
N-distal U=0.0 V
NO2
HNO2
NO
HNO
H2NO
H2NOH
NH2
NH3
Limiting potential results -1.83 V
Energy (eV)
Reaction
H+/e-
-H2O

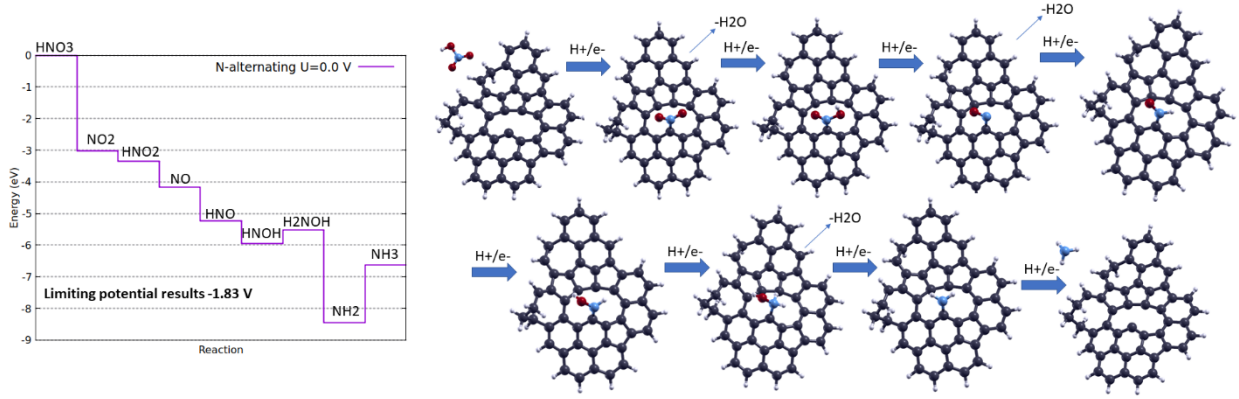
HNO3
N-alternating U=0.0 V
NO2
HNO2
NO
HNO
HNOH
H2NOH
NH2
NH3
Limiting potential results -1.83 V
Energy (eV)
Reaction
H+/e-
-H2O

Fig. S17. Energy diagrams and local minimum energy configurations of the NO_3RR mechanisms O-distal, O-alternating, N-distal, and N-alternaing taking place on the local defect site of the NDC material selected in the present investigation. Carbon atoms are grey, H white, O red, and N blue.

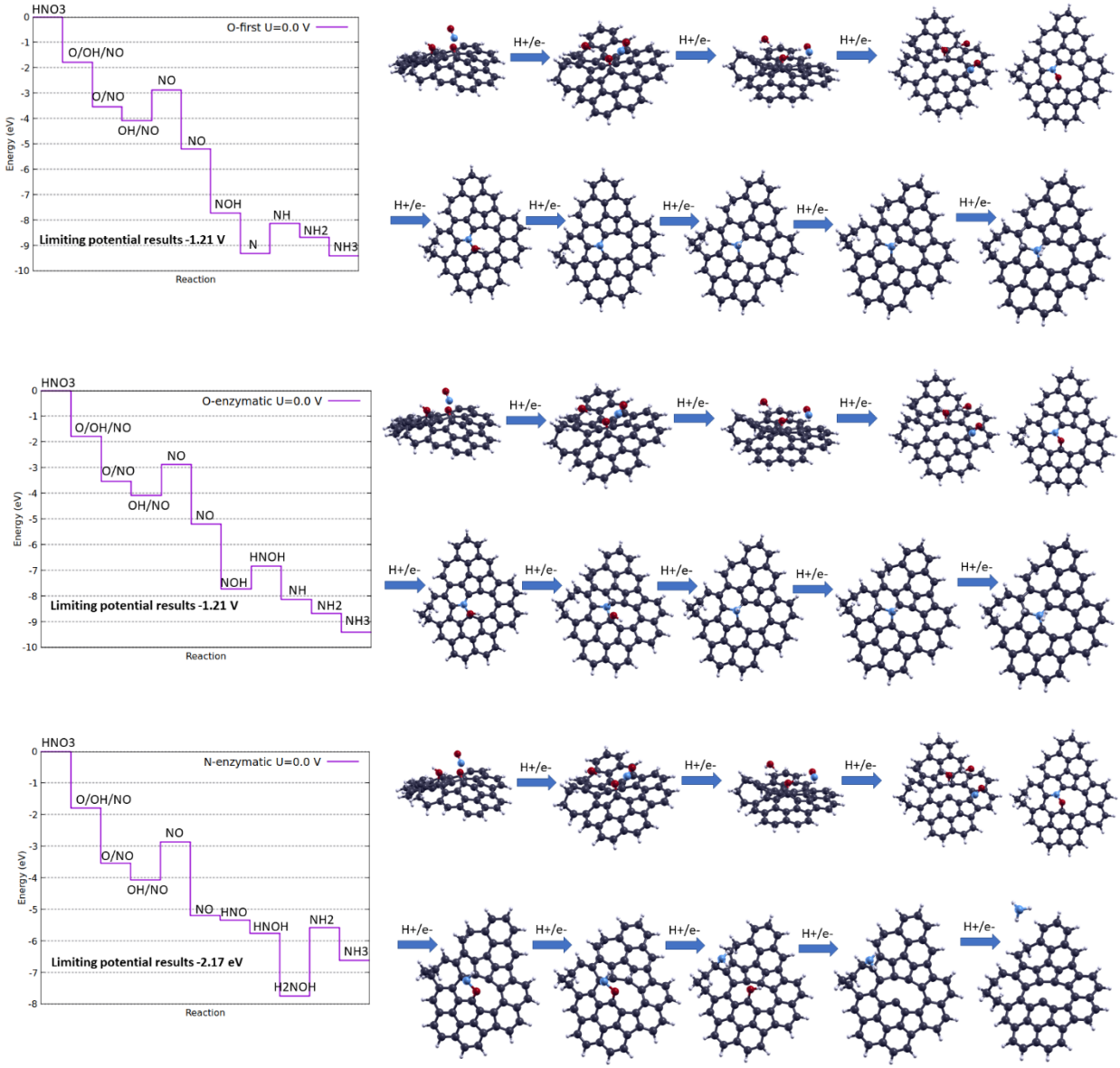

Fig. S18. Energy diagrams and local minimum energy configurations of the NO_3RR mechanisms O-first, O-enzymatic, and N-enzymatic taking place on the local defect site of the NDC material selected in the present investigation. The N-first mechanism is reported in the main paper. Carbon atoms are grey, H white, O red, and N blue.

Table S1 Comparison of Faradaic efficiency, Removal of NO_3^- and NH_4^+ selectivity of reported metal free electrocatalysts.

Electrocatalyst	Faradaic efficiency (%)	Removal of NO_3^-	NH_4^+ selectivity	Ref.
NDC-800	20.8	100 % in 48 h	73.1 % in 48 h	This work
N-doped graphene	–	4.4 % in 3 h	–	7
F-doped carbon	20	20 % in 10h	–	8
BDD	–	96.5 % in 4 h	8.8 %	9
BDD	–	91.0 % in 2 h	3.6 %	10

References

1 S. Monti, G. Barcaro, W. A. Goddard and A. Fortunelli, *ACS Nano*, 2021, **15**, 6369–6385.

2 C. Zhu, S. Monti and A. P. Mathew, *Carbohydr. Polym.*, 2020, **229**, 115510.

3 Scientific Computing & Modelling NV, *ADF Manual Amsterdam Modeling Suite 2019*, 2019.

4 P. Steve, *J. Comput. Physics,* 1995, **117**, 1–19.

5 A. Jurcik, D. Bednar, J. Byska, S. M. Marques, K. Furmanova, L. Daniel, P. Kokkonen, J. Brezovsky, O. Strnad, J. Stourac, A. Pavelka, M. Manak, J. Damborsky and B. Kozlikova, *Bioinformatics*, 2018, **34**, 3586–3588.

6 G. Gaussian 09, Revision A.02, M. J. Frisch, G. W. Trucks, H. B. Schlegel, G. E. Scuseria, M. A. Robb, J. R. Cheeseman, G. Scalmani, V. Barone, G. A. Petersson, H. Nakatsuji, X. Li, M. Caricato, A. Marenich, J. Bloino, B. G. Janesko, R. Gomperts, B. Mennucci, *Gaussian, Inc., Wallingford CT*.

7. J. Zhao, B. Shang and J. Zhai, *Nanomater.*, 2021, **11**, 2418.

8. Y. Li, S. Xiao, X. Li, C. Chang, M. Xie, J. Xu and Z. Yang, *Mater. Today Phys.*, 2021, **19**, 100431.

9. M. Ghazouani, H. Akrout and L. Bousselmi, *Desalin. Water Treat.,* 2015, **53**, 1107-1117.

10. M. Ghazouani, H. Akrout, S. Jomaa, S. Jellali and L. Bousselmi, *J. Electroanal. Chem.*, 2016, **783**, 28-40.